CHEMISTRY OF MATERIALS

pubs.acs.org/cm Article

# Rational Design of Heat-Resistant Polymers with Low Curing Energies by a Materials Genome Approach

Junli Zhu,[†] Ming Chu,[†] Zuowei Chen, Liquan Wang,* Jiaping Lin,* and Lei Du

Cite This: Chem. Mater. 2020, 32, 4527−4535

Read Online

ACCESS | Metrics & More | Article Recommendations | Supporting Information

ABSTRACT: Designing high-temperature polymers with excellent processability is a long-standing challenge because of the implacable contradiction between high thermal stability and low curing energy. Traditional designs based on scientific intuition and trial-and-error experiments have not been efficient strategies for the discovery of new heat-resistant resins. In this work, we developed a materials genome approach to facilitate the design of new heat-resistant resins with the desired properties. By defining the gene and extracting key features for properties, we proposed a two-step strategy to screen candidate resins obtained from combinations of genes. A new kind of heat-resistant resin was predicted by rapid screening and was further verified by theoretical simulations and experimental studies. The basic framework developed for the present materials genome approach can be generalized for the rapid design of other high-performance materials.

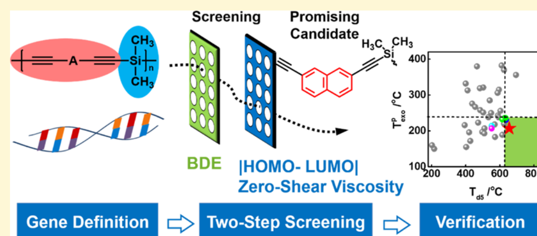


## ■ INTRODUCTION

Heat-resistant polymers and their composites have been widely used in aerospace, information, and electronic industries.[1−3] With the development of modern industries, a variety of heat-resistant polymers have been developed for use in long-term applications at elevated temperatures. New heat-resistant polymers are expected to have incredible thermal stability and excellent processability, but high thermal resistance in polymers is usually accompanied by undesirable poor processing characteristics, such as an extremely high curing temperature and large curing enthalpy. For example, polyimide and phthalonitrile resins, two well-known heat-resistant polymers, face a series of problems associated with their processing.[4−6] This contradictory relationship between high-temperature resistance and excellent processability has made the exploration and exploitation of new heat-resistant polymers a long-standing challenge.

The increasingly stringent requirements in terms of properties and processing conditions for future applications in the aerospace industry render the list of suitable resins currently available vanishingly small and limit the choices to a tiny number of heat-resistant resins. Silicon-containing arylacetylene resin, which possesses relatively better processability than polyimide and phthalonitrile resins with no deterioration at high temperatures, is a promising candidate for heat-resistant applications.[7] Resins of this kind, such as poly(silane arylacetylene) (PSA), were first exploited by Itoh et al.[8] and were further improved by Du et al.[9−11] Most silicon-containing arylacetylene resins decompose with 5% weight loss above 600 °C and have low viscosities (below 2 Pa·s) at their processing temperature. However, the thermal curing temperature and exothermic enthalpy of silicon-containing arylacetylene resins are usually higher than ca. 240 °C and ca. 350 J/g, respectively, which are unsuitable for the processing and manufacturing of high-performance composites.[12] The goal of this study is to identify new silicon-containing arylacetylene resins with high-temperature resistance and low curing energies (low curing temperatures and enthalpies).

The traditional design strategies based on scientific intuition and trial-and-error experiments are bound by high costs and time-consuming synthetic procedures. Therefore, a new paradigm for the design of these materials is of great importance for discovering advanced materials in a more efficient and economical way. A materials genome approach rooted in computation, experiments, and database searches could accelerate the development of advanced materials. Recently, materials genome approaches have been developed for discovering advanced materials, including new alloys[13] and inorganic materials.[14,15] However, it is challenging to develop a materials genome approach for polymers because of the fundamental obstacle in polymer discovery resulting from the immensely vast and complex chemical and morphological spaces of polymers. Recently, Ramprasad et al. established a materials genome approach to accelerate the discovery of on-demand polymers, such as polymer dielectrics.[16−20] Their works opened up opportunities for machine learning and

Received: January 19, 2020
Revised: May 13, 2020
Published: May 13, 2020

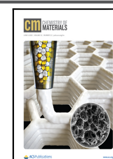

Downloaded via EAST CHINA UNIV SCIENCE & TECHLGY on October 22, 2020 at 14:26:13 (UTC).
See https://pubs.acs.org/sharingguidelines for options on how to legitimately share published articles.


© 2020 American Chemical Society

https://dx.doi.org/10.1021/acs.chemmater.0c00238
Chem. Mater. 2020, 32, 4527−4535

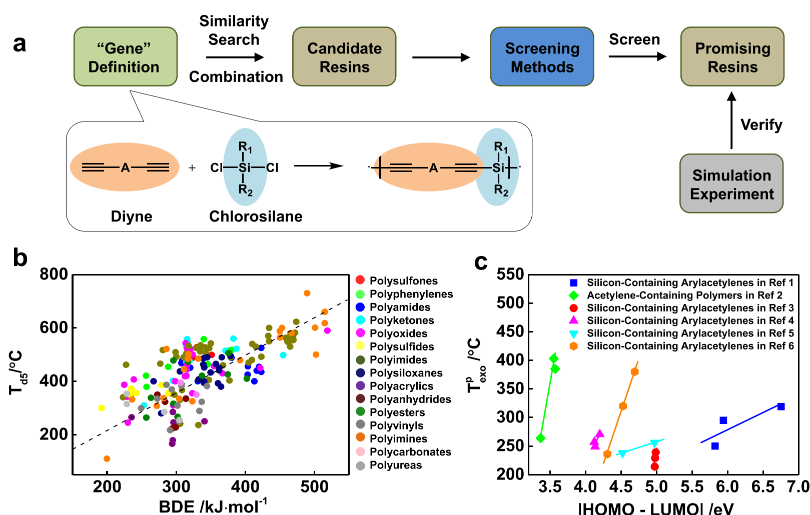


**Figure 1.** Gene definition and key features chosen for the materials genome method. (a) Screening approach for the rapid design of heat-resistant silicon-containing arylacetylene resins. (b) Correlation between 5% decomposition temperature and bond dissociation energy (BDE) of the weakest bond in polymers. The data of 5% decomposition temperatures are collected from the PoLyInfo database.[26] (c) Correlation between curing exothermic peak temperature in DSC curves and the |HOMO−LUMO| of various kinds of resins. The DSC data are collected from the literature listed in Section 2 of the Supporting Information.

informatics approaches in polymer design. Nevertheless, the materials genome approach for screening polymers with a variety of essential properties still need to be developed, especially for the cured resins with complicated three-dimensional cross-linked structures.

In this work, we applied a materials genome approach to the design of new heat-resistant and low-energy curing silicon-containing arylacetylene resins. Because heat-resistant polymers have more complex structures (such as chain connectivity and cross-linking) than most materials, developing a materials genome approach for screening resins with targeted properties is quite challenging. In the developed method, we first defined the "genes" of the resins and identified key features that are indicative of the thermal properties and curing properties by analyzing the available data. Then, we screened candidate resins using the key features that indicate the desired properties in a two-step manner. Density functional theory (DFT) and molecular dynamics (MD) simulations were used to verify the screening results. Finally, we experimentally synthesized the screened resins that were expected to have excellent combinations of high-temperature resistance and lower curing energy. The thermal decomposition (5% weight loss) of the synthesized resin occurs at 655 °C, and the exothermic peak with a much lower curing enthalpy (241.9 J/g) appears at 207 °C. The agreement between the screening results and experimental observations demonstrates the validity of the materials genome approach, which could be further applied in the design of other advanced materials.

## ■ RESULTS AND DISCUSSION

**Definition of Genes in Silicon-Containing Arylacetylene Resins.** The first task in constructing a materials genome method is defining the genes of silicon-containing arylacetylene resins. In biology, a gene is a sequence of nucleotides in the DNA or RNA that codes for a functional molecule. Gene sequences and genetic codes are the two main themes. When applying the concept of a gene to the field of polymers, the gene sequence and genetic code can refer to the structure and structure−property relationship of the polymer.[21] From a structural perspective, the gene sequence of a polymer can be expressed as the sequence of chemical units that construct the polymer. Moreover, the polymer chains can also cross-link to form polymer networks.

In general, chemical groups such as $-CH_2-$, $-CO-$, $-O-$, and $-C_6H_4-$ can be considered as the genes that make up polymer chains following a specific sequence.[17,20] Such a definition allows structural design in vast chemical space, but it makes the synthesis quite challenging. To balance the flexibility of the structure design with the practical challenges of experimental synthesis, we defined the genes of silicon-containing arylacetylene resins in terms of synthetic routes.[22] Silicon-containing arylacetylene resins can be synthesized via (1) a reduction with Zn and (2) a Grignard reaction.[23,24] In these synthetic routes, diynes and chlorosilanes are necessary reactants (see Figure 1a). As such, silicon-containing arylacetylene can be expressed as a combination of two essential genes. The first kind of gene is derived from one diyne monomer containing two alkynyl groups ($-C{\equiv}C-A-C{\equiv}C-$, where A is the chemical group connecting the two alkyne units), and the second kind of gene includes the Si moiety, which is derived from a chlorosilane ($-Si(R_1)(R_2)-$) in which $R_1$ and $R_2$ are substituents connected to the Si atom. Either of these genes can be altered to construct a new polymer, but herein, we only focused on the diyne "genes" and fixed the chlorosilane "genes" as dichlorodimethylsilane because ample chemical space is available for the design of the diyne, and they are practically synthetically accessible. Before the screening, a series of diynes with various chemical structures were collected from the available chemical databases, including SciFinder, ChemSpider, and PubChem. Similarity searches, as well as downloading and processing of the molecules, were performed through the application program interface of each database and RDKit software.[25]

Once each polymer chain was represented as a sequence of genes, high-throughput screening can then be implemented with a specific "genetic code", that is, the structure−property relationships. We attempted to optimize the following properties by structural design: heat resistance, curing

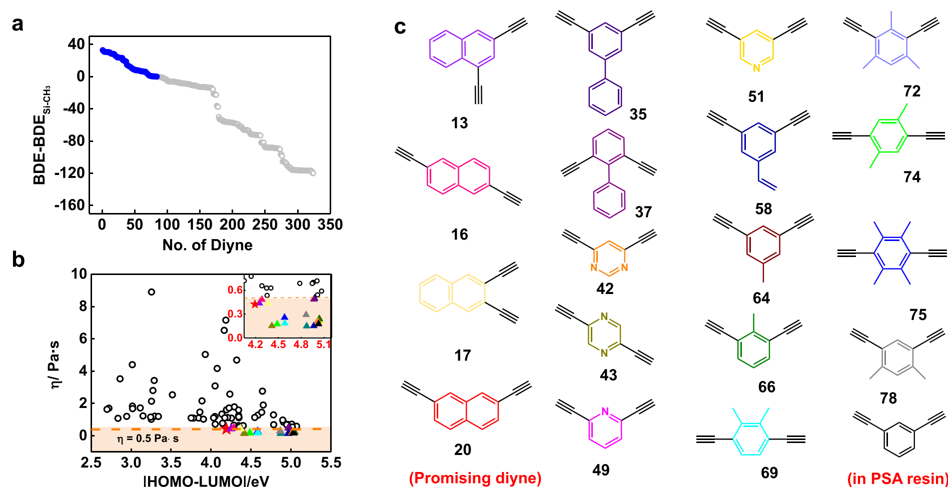


**Figure 2.** Two-step computational high-throughput screening of heat-resistant resins. (a) First-step screening: plot of the difference between the BDE of the weakest bond in candidate resins and the BDE of Si−$CH_3$ vs the number of candidate diynes. Data points above the screening criterion of BDE are distinguished with a blue color. (b) Second-step screening: plot of zero-shear viscosity vs the |HOMO−LUMO| of the 84 candidate resins. The dashed line denotes the zero-shear viscosity threshold $\eta$ = 0.5 Pa·s. (c) Structures of the candidate diynes that meet the requirement of zero-shear viscosity in the second-step screening.

temperature, and viscosity. Heat resistance is essential for silicon-containing arylacetylene resins. Improving the heat resistance of a resin can broaden its application scope in aerospace and astronautics. Curing temperature is associated with the processing conditions. A low curing temperature can reduce the cost and inconvenience associated with the processing[12] and decrease the internal stress caused by cross-linking. The viscosity of silicon-containing arylacetylene resins is fairly low compared with those of polyimide and phthalonitrile resins. However, improving the thermal stability often makes processing more difficult (e.g., high curing temperature and high viscosity at the processing temperature) (for an example, see Figure S2), which limits the applicability of many heat-resistant resins. Therefore, we included the viscosity of the resin as a screening criterion to ensure that the identified resins were suitable for processing methods such as resin-transfer molding (RTM).

Because it is challenging to explore the "genetic code" of silicon-containing arylacetylene resins, that is, to reveal the quantitative relationship between polymer structures and properties such as heat resistance and curing temperature, we identified key features that characterize heat resistance and curing temperature by analyzing existing experimental and computational data. We collected the 5% decomposition temperatures ($T_{d5}$ values) of more than 400 polymers from the PoLyInfo database[26] and then plotted the $T_{d5}$ values versus the bond dissociation energy (BDE) of the weakest bond in the structure of each polymer. The resulting plot is shown in Figure 1b. As shown, the heat resistance of the resin is closely related to its BDE, where the Pearson correlation value is ca. 0.68. A high BDE generally improves the heat resistance of the polymer, resulting in a high value of $T_{d5}$. The molecular weight and location of the weakest bond in the structure have smaller effects on the heat resistance of the polymer. Therefore, the BDE can be considered a key feature for evaluating thermal stability for genes.

The |HOMO−LUMO| gap between the highest occupied molecular orbital (HOMO) and lowest unoccupied molecular orbital (LUMO) is usually used to predict the reactivity of a molecule. We also analyzed the curing conditions of acetylene-containing polymers (the data are collected from the literature listed in Section 2 of the Supporting Information) and plotted their curing exothermic peak temperatures ($T_{exo}^{p}$ values) obtained from differential scanning calorimetry (DSC) curves versus the |HOMO−LUMO| (calculated by DFT) for various kinds of resins, and the resulting plot is shown in Figure 1c. The positive correlation between $T_{exo}^{p}$ and the |HOMO−LUMO| shown in the figure suggests that the |HOMO−LUMO| can be used as a key feature for evaluating the curing temperature. Notably, we used the |HOMO−LUMO| to compare the reactivities of the reactants with the same reactive groups and similar constituents so that other factors influencing the activation energy can be ignored.[27,28] The identification of these two key features enabled fast calculations and, therefore, high-throughput screening. Unlike the properties of heat resistance and curing temperature, the relationship between the chemical structure and zero-shear viscosity can be directly established by a group contribution method.[29] We have tested the validity of the group contribution method in predicting the viscosity of heat-resistant polymers, such as silicon-containing arylacetylene resins and polyimides, with a broad range of viscosities varying from 0.0623 to 9 Pa·s. The results demonstrate that the model is valid for predicting the zero-shear viscosities of silicon-containing arylacetylene resins (see Figure S1).

**Two-Step Screening of New Silicon-Containing Arylacetylene Resins.** We proposed a two-step strategy to rapidly design and screen new silicon-containing arylacetylene resins with high-temperature resistance and excellent processability (see Figure 1a). Before the high-throughput screening, a library of 324 diynes was collected from chemical databases (for detailed structures, see Section 5 of the Supporting Information). The diynes were combined with dichlorodimethylsilane to generate a series of candidate resins. Subsequently, the first step of the screening was performed based on BDE as a key feature. The BDEs of the weakest bonds in the candidate resins were calculated by DFT (for the detailed method, see Section 1 of the Supporting Information). Because we calculated the BDE of the bond in the repeating unit of a polymer chain, the molecular structure of the resin in

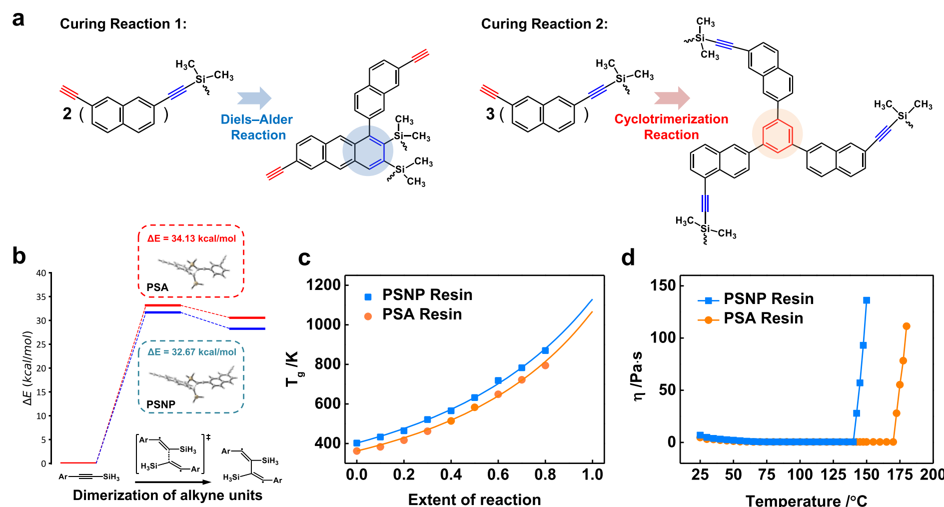


**Figure 3.** Simulation verification of the screening results. (a) Cross-linking reactions of alkyne units considered in the MD simulations: Diels–Alder reaction and cyclotrimerization reaction. The cured structures formed by Diels–Alder reaction and cyclotrimerization reaction are marked with blue and red areas, respectively. (b) Activation energies of silicon-containing arylacetylene resins containing 1,3-diethynylbenzene (red) and 2,7-diethynylnaphthalene (blue). (c) Glass-transition temperatures of the PSNP and PSA resins as a function of the extent of reaction. (d) Viscosities of the PSNP and PSA resins as a function of temperature.

the calculation corresponds to a polymer chain. Figure 2a shows the calculated BDEs for the 324 candidate resins. In the figure, we have sorted the diyne "genes" by their BDE in descending order and given each a corresponding sequence number. We then defined a threshold of 372 kJ/mol for this screening. This threshold value is the lowest BDE of the Si–$CH_3$ bond in the backbone of a well-known PSA resin.[30,31] If the BDE of the weakest bond is higher than that of Si–$CH_3$, the thermal stability of the candidate resin could be better than that of PSA. As such, the candidate resins containing bonds with BDEs lower than 372 kJ/mol were eliminated in the first step of this screening. After applying the BDE as a constraint for these candidate resins, the number of potential candidates was decreased from 324 to 84.

We continued to conduct the second step of the screening by using the second key feature for curing temperatures (i.e., |HOMO–LUMO|) and the zero-shear viscosity as constraints on the remaining 84 candidate resins. The |HOMO–LUMO|s and zero-shear viscosities of the candidate resins were calculated by DFT and the group contribution method. As shown in Figure 2b, we plotted the zero-shear viscosities of the candidate resins as a function of their |HOMO–LUMO|s. For RTM, which is widely used for manufacturing high-performance composites, the optimum viscosity is approximately 0.1–0.5 Pa·s, and the mold pressures are difficult to handle for resins with a viscosity higher than 0.5 Pa·s.[32] We, therefore, used a zero-shear viscosity lower than 0.5 Pa·s as a threshold to screen candidate resins. The zero-shear viscosity threshold can immediately eliminate a portion of the candidate resins (those above the dashed line in Figure 2b), and 18 structures remained after this step. We then selected the resin with the smallest |HOMO–LUMO| among the remaining structures (the molecular structures are shown in Figure 2c) as the most promising resin. 2,7-Diethynylnaphthalene is a target gene for constructing promising resins with an excellent combination of properties. The screened resins containing 2,7-diethynylnaphthalene were named PSNP resins.

**Theoretical Verification of the Properties of the Screened Resins.** We performed theoretical simulations to judge whether the PSNP resins would have higher temperature resistance and better curing properties than PSA resins. DFT calculations and MD simulations were first carried out to elucidate the reaction activation energies and thermal properties of the PSNP resins and the original PSA resin.

The activation energies of the curing reactions for the PSNP and PSA resins were calculated by DFT to determine if the PSNP resins could be cured at a lower temperature. The dimerization of two alkyne units is the rate-determining step in the curing reactions of the PSNP and PSA resins, such as cyclotrimerization and Diels–Alder reactions (see Figure 3a).[33−36] We, therefore, calculated the activation energies of the dimerization of two alkyne units for the PSNP and PSA resins. The transition states were searched, and the activation energies were obtained (see Figure 3b). As shown, the activation energies of the PSNP and PSA resins are 32.67 and 34.13 kcal/mol, respectively. The lower activation energy in the reaction of the PSNP resins indicates that the curing temperature could be lowered by substituting 1,3-diethynylbenzene for 2,7-diethynylnaphthalene.

Because the silicon-containing arylacetylene resin is highly cross-linked, it is challenging to characterize the $T_g$ using existing instruments such as DSC.[37] For linear polymers, the $T_g$ can now be well predicted by the surrogate models constructed through data-driven methods such as the machine learning method.[16−18,38] For the cross-linked polymers, however, the degree of curing should be included in the prediction model. Because the present work centers on the PSA and PSNP resins, we employed MD simulations to obtain the glass-transition temperatures of the cured resins instead of developing surrogate models.

A cross-linking approach based on a cutoff distance criterion and a multistep relaxation procedure was used to mimic the curing reaction of silicon-containing arylacetylene resins (for details, see the Methods section and Figure S3). Cyclotrimerization and Diels–Alder reaction between alkynyl groups were considered in the curing procedure,[39] as shown in Figure 3a. We obtained the glass-transition temperatures by examining the variation in density as a function of temperature.


https://dx.doi.org/10.1021/acs.chemmater.0c00238
Chem. Mater. 2020, 32, 4527−4535

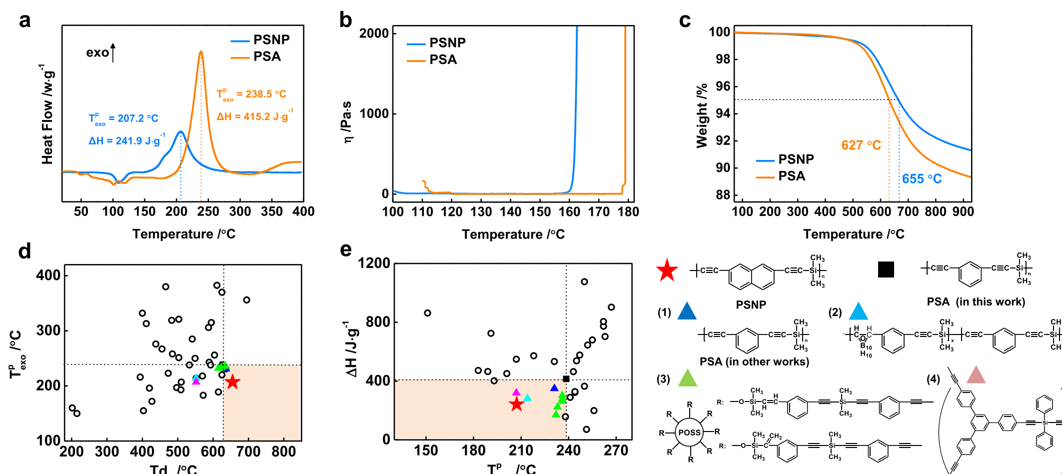


Figure 4. Experimental verification of the computational screening results. (a) DSC curves (10 °C/min in $N_2$) of the PSNP and PSA resins. (b) Plots of viscosity as a function of temperature for the PSNP and PSA resins. (c) TGA curves (10 °C/min in $N_2$) of the cured PSNP and PSA resins. (d) Plot of curing exothermic peak temperature vs 5% decomposition temperature. (e) Plot of curing exothermic enthalpy vs curing exothermic peak temperature. The chemical structures of the resins for the solid points in (d,e) are listed in the right side of (e). Except for the thermal results of the PSNP and PSA resins, other data in (d,e) are collected from the literature listed in Section 21 of the Supporting Information.

The dependence of the density on temperature can show an abrupt change, which is usually used to determine the glass-transition temperature.[40] The glass-transition temperatures of the resins were plotted as a function of conversion, as shown in Figure 3c. One can see that replacing the 1,3-diethynylbenzene gene with 2,7-diethynylnaphthalene can increase the glass-transition temperature.

The glass-transition temperatures ($T_g^\infty$ values) of the fully cured resins were predicted to be 857 and 795 °C for the PSNP and PSA resins, respectively, by fitting the simulation data with the Venditti−Gillham equation[41] and extrapolating (for details, see section 8 of the Supporting Information). The increase in $T_g^\infty$ indicates that the new PSNP resins could be more temperature-resistant than the PSA resins. The elevation in the $T_g^\infty$ of PSNP can be attributed to the increased fraction of ring structures in the polymer. The ring structures are found to be positively correlated with the $T_g$ because the rings can increase the stiffness of the polymer chain and reduce the mobility of the segments.[16] For most heat-resistant thermosetting resins, there is a positive correlation between their 5% thermal decomposition temperatures and their glass-transition temperatures (see Figure S4). The elevated $T_g$ values indicate that the resistance to thermal decomposition is improved. The simulation observations support the screening results that replacing 1,3-diethynylbenzene with 2,7-diethynylnaphthalene can improve the thermal stability of silicon-containing arylacetylene resins.

We also calculated the viscosities of the PSA and PSNP resins by MD simulations. Because the cross-linking reaction occurs during curing, it is challenging to determine the viscosity of the resins during the curing process by MD simulations. We, therefore, developed a simulation method combining the curing reaction and nonequilibrium MD simulations for studying the variation of viscosity during the curing of silicon-containing arylacetylene resins (for details of the method, see Section 10 of the Supporting Information). Figure 3d shows the viscosities as a function of temperature. The viscosity first decreases and then increases with increasing temperature. The onset of the increase in viscosity corresponds to the curing reaction. The viscosity of the PSNP resin is slightly higher than that of the PSA resin, which is in agreement with the zero-shear viscosities calculated for these two resins in the computational screening (0.4242 Pa·s for the PSNP resin and 0.1773 Pa·s for the PSA resin, as shown in Figure 2b). The viscosity of the PSNP resin, which is lower than those of common polyimide and phthalonitrile resins, makes it suitable for most processing methods, such as RTM.

**Experimental Verification of the Screening Results.** We finally presented a proof-of-concept experiment aimed at testing the validity of our materials genome method. 2,7-Diethynylnaphthalene was synthesized, and the corresponding silicon-containing arylacetylene resin (PSNP resin) was prepared by a Grignard reaction between dimethyldichlorosilane and 2,7-diethynylnaphthalene.[42] For comparison, the PSA resins were also prepared using the method described in our previous works.[39] The PSNP and PSA resins were both thermally cured with the same procedure (the details are given in the Methods section).

We characterized the thermal curing behaviors of the PSNP and PSA resins by DSC, and the DSC curves are shown in Figure 4a. The DSC profile of conventional PSA resins showed an exothermic transformation of the thermal curing reaction in the range of 214−256 °C, and the peak was observed at 238 °C. In the DSC profile of the PSNP resins, the exothermic area of the thermal curing reaction is shifted to a lower temperature range (178−234 °C) with a peak at 207 °C. As such, the curing reaction of the PSNP resins could be conducted at a lower temperature than that of the PSA resins. Such an advantage results from the replacement of 1,3-diethynylbenzene with 2,7-diethynylnaphthalene. Moreover, the curing enthalpy of the PSNP resin is 241.9 J/g, which is 173.3 J/g lower than that of the PSA resin (415.2 J/g).

The apparent activation energies for curing of the PSA and PSNP resins, obtained from DSC curves, were compared with DFT results (for the detailed method, see Section 19 of the Supporting Information). The results are presented in Table S6. Both the experiments and DFT computations show that the activation energy for the curing of the PSNP is significantly lower than that of the PSA resin, which verifies the screening results. The activation energies obtained from experiments are

lower than those computed by the DFT. This is because the DFT computations center only on the internal alkynes whose reactivity could be lower than that of terminal alkyne. Moreover, only the rate-determining step, that is, the dimerization of two alkyne units, was considered in the DFT computations. The computation results could overestimate the activation energy because other types of curing reactions, such as Glaser coupling and Strauss coupling reactions, can lower the apparent activation energy in the experiments.

Figure 4b shows the viscosity of the PSNP resin as a function of temperature. With increasing temperature, the PSNP resin gradually melts, and the viscosity decreases. As the temperature increases beyond 140 °C, the alkynyl groups react with each other, and the resin begins to cross-link, which leads to a dramatic increase in viscosity. Moreover, the viscosity of the melting PSNP resin is comparable to that of the PSA resins. The window for processing is larger than 60 °C, which is suitable for most processing methods. Notably, the experimental and simulation results drew the same conclusion that the viscosity of the PSNP resin is higher than that of the PSA resin, which agrees with the screening results. On a quantitative level, the experimental viscosities of PSA and PSNP resins at processing temperatures are in the range of 0.2634−0.6837 Pa·s and 0.4727−0.8953 Pa·s, respectively. The simulation viscosities of PSA and PSNP resins are lower than the experimental viscosities, which are 0.019 and 0.027 Pa·s, respectively (Figure 3d). The difference arises because the experimental viscosities approach the zero-shear viscosities predicted in the screening procedure, while the simulation corresponds to the case with a high shear rate. Moreover, the MD simulation does not take into account the effect of the molecular weight distribution.[43]

Thermogravimetric analysis (TGA) was finally performed to reveal the thermal stability of the new PSNP resins. Figure 4c shows the TGA curves of the cured PSA and PSNP resins. Under a nitrogen atmosphere, both of these resins tolerate high temperatures with little mass loss until 550 °C. The cured PSNP resins decompose with 5% weight loss at 655 °C, that is, $T_{d5}$ = 655 °C. This $T_{d5}$ is higher than that (627 °C) of the cured PSA resins. The residual yield at 800 °C is 92.3%, which is larger than that (90.3%) of the cured PSA resins. The TGA results indicate that the presence of the naphthyl "gene" in the backbone improves the thermal stability. We found that the positive correlation between the BDE and thermal stability can apply to the PSA and PSNP resins. The BDE of the weakest bond of PSNP is 19.93 kJ/mol higher than that of PSA. Accordingly, the 5% thermal decomposition temperature of PSNP is 28 °C higher than that of PSA. This comparison can validate our screening method for thermal stability. Because there is a positive correlation between $T_{d5}$ and $T_g$ for heat-resistant resins (Figure S4), the experimental results of $T_{d5}$ can be in correspondence with the simulation results of $T_g$; that is, the PSNP resins can have both a high $T_{d5}$ and $T_g$.

To highlight the advantages of the present materials, we compared the properties of the PSNP resins to the properties of similar resins currently available (silicon-containing arylacetylene resins cured by alkyne units). We first plotted the curing exothermic peak temperatures ($T^{p}_{exo}$ values) against $T_{d5}$ (see Figure 4d, note that the data were collected from the literature listed in Section 21 of the Supporting Information). Only the PSNP resin (indicated by the red star) exhibits a combination of properties superior to those of the PSA resins; that is, the PSNP resin possesses a higher $T_{d5}$ and a lower $T^{p}_{exo}$ than the PSA resins. We then plotted the curing enthalpy ($\Delta H$) vs $T^{p}_{exo}$ (see Figure 4e). Five types of arylacetylene resins, including PSNP resins, exhibit lower $T^{p}_{exo}$ and $\Delta H$ values than the PSA resins. Considering the data in both Figure 4d,e, the PSNP resins exhibit the most desirable combination of properties, that is, a higher $T_{d5}$, a lower $T^{p}_{exo}$, and a lower $\Delta H$ compared to the PSA resins. The new resins designed herein offer both high-temperature resistance and low curing energy.

Finally, we aimed to provide an intuitive explanation for why PSNP resins exhibit better comprehensive properties than the original PSA resins. The structural difference between PSNP and PSA is the alkyne-containing groups, where PSNP and PSA include naphthalene and benzene, respectively. Notably, there are four candidates containing a naphthalene ring among the 18 down-selected candidates with excellent thermal stability and low viscosity. The resin containing 1,3-diethynylnaphthalene or 2,6-diethynylnaphthalene could be another promising resin besides the PSNP (see Figure 2c), which implies the advantage of naphthalene in designing heat-resistant resins. The donor ability of the substituent attached to the alkynyl unit has a substantial influence on the dimerization of arylacetylenes.[44] Compared with benzene, the enhanced donor character of naphthalene can reduce the activation barrier of the dimerization and stabilize the diradical intermediates, leading to a decrease in the curing temperatures. Because of the introduction of the naphthalene ring, the weight fraction of reacted alkyne groups in the PSNP was reduced, which leads to the low curing enthalpy of the PSNP. Moreover, the naphthalene ring is more thermally stable than other chemical units in the PSA and PSNP resins because of its high BDEs. The introduction of the naphthalene ring reduces the weight fraction of weakly bound units (especially $Si-CH_3$) in the PSNP resins, resulting in a higher $T_{d5}$ than that of the PSA. However, thermally stable units are usually associated with rigid chemical structures and higher molecular weights, which can lead to higher viscosity, such as the case in the PSNP resin. In this work, the best balance between thermal stability and processability was found with silicon-containing arylacetylene resins.

## ■ CONCLUSIONS

In summary, we have addressed the apparent contradiction between the high thermal stability and poor processability of heat-resistant resins by a rapid screening strategy and presented an example of how a materials genome method can be used in the rapid design of low-energy curing and heat-resistant silicon-containing arylacetylene resins. A new kind of silicon-containing arylacetylene resin was developed by a combinatorial design and high-throughput screening, and it was further verified by theoretical simulations and experimental studies. The developed materials genome method involves two key points. The first is the rule of dividing the polymers into genes. We defined the genes according to the chemical synthesis rules to guarantee that the designed products were synthetically accessible. The second is to extract key features for properties from the available data. We obtained two key features, the BDE and |HOMO−LUMO|, which can indicate the thermal stability and curing behavior of the resins, thus facilitating the high-throughput screening of the candidate resins. We have theoretically and experimentally confirmed the prediction that the screened resins have high-temperature resistance and low curing energies. This work demonstrated that the present materials genome approach is a promising


https://dx.doi.org/10.1021/acs.chemmater.0c00238
Chem. Mater. 2020, 32, 4527−4535

strategy for the computational screening of heat-resistant resins. The success of this materials genome method will not only accelerate the discovery of new heat-resistant resins but also provide a new platform for the design and development of other high-performance materials.

## ■ METHODS

**Screening Method.** (1) Data set: All of the chemical structures with their "genetic" characteristics were searched for in the SciFinder, ChemSpider, and PubChem databases using the Tanimoto similarity algorithm[45] and downloaded in batches through the application programming interfaces (APIs) of the databases. (2) First-step screening: the candidates obtained from the combination of genes were first screened based on the key feature of BDE (Section 1 of the Supporting Information). The structures with weak bonds were eliminated to guarantee that the cured resin can resist thermal decomposition at high temperatures. (3) Second-step screening: the zero-shear viscosity and the |HOMO−LUMO| were evaluated for the resins that remained after the first step of the screening process. The zero-shear viscosities of the candidate resins with a degree of polymerization of 4 were calculated in the Synthia modulus of Materials Studio[46] using a group addition method (Section 3 of the Supporting Information). The |HOMO−LUMO| values were calculated with Gaussian 09 software at the B3LYP/6-311G(d,p) level.[47]

**Validation of the Screening Results by Simulation.** MD simulations[48,49] (for details, see Section 6 of the Supporting Information) were performed to understand the thermal properties of the cured arylacetylene resins. A cross-linking approach based on a cutoff distance criterion and a multistep relaxation procedure was designed and used to construct the polymer networks.[50−54] A flowchart is shown in Figure S3. The procedure, including the formation of new bonds, geometry optimization, and MD simulations under the *NPT* and *NVT* ensembles, was realized with Materials Studio. The Andersen thermostat and the Berendsen barostat were applied to control the temperature and pressure, respectively. The COMPASS force field was adopted throughout the simulations.[55] Both the van der Waals forces and Coulomb forces with a cutoff of 12.5 Å were calculated by an atom-based summation method. The time step was set to 1.0 fs.

To validate the screening results of the |HOMO−LUMO|, the activation energies of the curing reactions for PSNP and PSA resins were calculated by DFT with the Gaussian 09 program package. Hybrid nonlocal DFT at the B3LYP level with the 6-31G(d,p) basis set was used to locate all the stationary points, that is, reactants, transition states, intermediates, and products.

**Experimental Verification of the Screening Results.** *Materials.* Tetrahydrofuran (THF), triethylamine, toluene, dichloromethane, *n*-hexane, silica gel, methyl alcohol, potassium carbonate, and concentrated hydrochloric acid were purchased from Titan Co. Ltd. Cuprous iodide and dimethyldichlorosilane were purchased from Aldrich Co. Ltd. 2,7-Dibromonaphthalene and trimethylsilylacetylene were purchased from Bide Pharmatech Ltd. Ethylmagnesium bromide (1.0 M in THF) was purchased from J&K Chemical Ltd. All experiments were conducted under strict anaerobic and anhydrous conditions.

*Sample Characterization.* $^1$H NMR spectra were acquired at 400 MHz (Bruker AVANCE 500) with $CDCl_3$ as the solvent. Elemental analysis was performed on a Vario EL III elemental analyzer. Chemical structures were characterized by an FT-IR instrument (Nicolet 6700). The viscosity of the resin was obtained by a rotational rheometer (RheoStress RS600). The curing behavior of the resin was characterized by a differential scanning calorimeter (TA, Q2000, 10 °C/min as the heating rate, under an $N_2$ atmosphere). The thermal properties were measured on a thermal gravimetric analyzer (TA, SDT Q600, 10 °C/min as the heating rate).

2,7-Diethylnaphthalene was synthesized via two steps: 1) 2,7-bis((trimethylsilyl)acetylene) naphthalene was synthesized by a Sonogashira coupling reaction, and 2,7-diethynylnaphthalene was obtained by the deprotection of 2,7-bis((trimethylsilyl) acetylene) (for details, see Section 11 of the Supporting Information). The structure of 2,7-diethynylnaphthalene was confirmed by $^1$H NMR spectroscopy, mass spectrometry, and elemental analysis, as shown in Figures S6 and S7 and Table S1. The PSNP resin was prepared by a Grignard reaction between 2,7-diethynylnaphthalene and dimethyldichlorosilane using THF as the solvent according to the reported method[42] (for details, see Section 13 of the Supporting Information). The PSNP resin was structurally characterized by $^1$H NMR spectroscopy and FT-IR spectroscopy, and the spectra are shown in Figures S9 and S10. The features of the PSNP resins, such as solubility and gelation time, are shown in Tables S2 and S3. The PSA resin was prepared by the method used in our previous works.[39] The PSNP and PSA resins were thermally cured according to the following procedures: 180 °C for 2 h, 220 °C for 2 h, 240 °C for 2 h, and 260 °C for 2 h. Other curing procedures were also tested, and the thermal properties of the cured resins are shown in Table S4. The DSC and TGA results of the cured PSNP and PSA resins are shown in Tables S5 and S7. The structural changes in the PSNP resins during curing were analyzed by FT-IR spectroscopy, and the spectra are shown in Figures S11 and S12.

## ■ ASSOCIATED CONTENT

### Supporting Information

The Supporting Information is available free of charge at https://pubs.acs.org/doi/10.1021/acs.chemmater.0c00238.

Calculation of BDE, prediction of zero-shear viscosities, plots of glass-transition temperature versus melt viscosity of polymers, chemical structures of 324 diynes, MD simulations and simulation procedure for resin curing, fitting model of $T_g$, plots of $T_g$ versus $T_{d5}$, viscosity calculation using nonequilibrium MD simulations, synthesis and structural characterization of 2,7-diethynylnaphthalene and PSNP resin, solubility and gelation time of PSNP resin, effects of curing procedures, structural changes during curing, DSC results of PSNP and PSA resins, TGA results of cured PSNP and PSA resins, and a list of the literature that provides the data for Figures 1c and 4d,e (PDF)

## ■ AUTHOR INFORMATION


### Corresponding Authors

**Liquan Wang** − *Shanghai Key Laboratory of Advanced Polymeric Materials, Key Laboratory for Ultrafine Materials of Ministry of Education, School of Materials Science and Engineering, East China University of Science and Technology, Shanghai 200237, China;* orcid.org/0000-0002-5141-8584; Phone: +86-21-64253370; Email: lq_wang@ecust.edu.cn

**Jiaping Lin** − *Shanghai Key Laboratory of Advanced Polymeric Materials, Key Laboratory for Ultrafine Materials of Ministry of Education, School of Materials Science and Engineering, East China University of Science and Technology, Shanghai 200237, China;* orcid.org/0000-0001-9633-4483; Email: jlin@ecust.edu.cn

### Authors

**Junli Zhu** − *Shanghai Key Laboratory of Advanced Polymeric Materials, Key Laboratory for Ultrafine Materials of Ministry of Education, School of Materials Science and Engineering, East China University of Science and Technology, Shanghai 200237, China*

**Ming Chu** − *Shanghai Key Laboratory of Advanced Polymeric Materials, Key Laboratory for Ultrafine Materials of Ministry of Education, School of Materials Science and Engineering, East*

China University of Science and Technology, Shanghai 200237, China
**Zuowei Chen** − *Shanghai Key Laboratory of Advanced Polymeric Materials, Key Laboratory for Ultrafine Materials of Ministry of Education, School of Materials Science and Engineering, East China University of Science and Technology, Shanghai 200237, China*
**Lei Du** − *Shanghai Key Laboratory of Advanced Polymeric Materials, Key Laboratory for Ultrafine Materials of Ministry of Education, School of Materials Science and Engineering, East China University of Science and Technology, Shanghai 200237, China*

Complete contact information is available at:
https://pubs.acs.org/10.1021/acs.chemmater.0c00238

### Author Contributions

†J.Z. and M.C. contributed equally.

### Notes

The authors declare no competing financial interest.

## ■ ACKNOWLEDGMENTS

This work was supported by the National Natural Science Foundation of China (51833003, 21975073, and 21774032). Support from the Project of Shanghai Municipality (16520721900) and the Fundamental Research Funds for the Central Universities (50321041918013) is also appreciated.

## ■ REFERENCES

(1) Critchley, J. P.; Knight, G. J.; Wright, W. W. *Heat-Resistant Polymers*; Plenum Press: New York, 1983.
(2) Li, Q.; Chen, L.; Gadinski, M. R.; Zhang, S.; Zhang, G.; Li, H. U.; Iagodkine, E.; Haque, A.; Chen, L.-Q.; Jackson, T. N.; Wang, Q. Flexible High-Temperature Dielectric Materials from Polymer Nanocomposites. *Nature* **2015**, *523*, 576−579.
(3) Kaltenbrunner, M.; Sekitani, T.; Reeder, J.; Yokota, T.; Kuribara, K.; Tokuhara, T.; Drack, M.; Schwödiauer, R.; Graz, I.; Bauer-Gogonea, S.; Bauer, S.; Someya, T. An Ultra-Lightweight Design for Imperceptible Plastic Electronics. *Nature* **2013**, *499*, 458−463.
(4) Liaw, D.-J.; Wang, K.-L.; Huang, Y.-C.; Lee, K.-R.; Lai, J.-Y.; Ha, C.-S. Advanced Polyimide Materials: Syntheses, Physical Properties and Applications. *Prog. Polym. Sci.* **2012**, *37*, 907−974.
(5) Keller, T. M.; Dominguez, D. D. High Temperature Resorcinol-Based Phthalonitrile Polymer. *Polymer* **2005**, *46*, 4614−4618.
(6) Laskoski, M.; Dominguez, D. D.; Keller, T. M. Synthesis and Properties of Aromatic Ether Phosphine Oxide Containing Oligomeric Phthalonitrile Resins with Improved Oxidative Stability. *Polymer* **2007**, *48*, 6234−6240.
(7) Shen, Y.; Yuan, Q.; Huang, F.; Du, L. Effect of Neutral Nickel Catalyst on Cure Process of Silicon-Containing Polyarylacetylene. *Thermochim. Acta* **2014**, *590*, 66−72.
(8) Itoh, M.; Inoue, K.; Iwata, K.; Ishikawa, J.; Takenaka, Y. A Heat-Resistant Silicon-Based Polymer. *Adv. Mater.* **1997**, *9*, 1187−1190.
(9) Li, F.; Wang, C.; Shen, X.; Huang, F.; Du, L. Synthesis and Characterization of Novel Silicon-Containing Aromatic Bispropargyl Ether Resins and Their Composites. *Polym. J.* **2011**, *43*, 594−599.
(10) Li, Q.; Zhou, Y.; Hang, X.; Deng, S.; Huang, F.; Du, L.; Li, Z. Synthesis and Characterization of a Novel Arylacetylene Oligomer Containing POSS Units in Main Chains. *Eur. Polym. J.* **2008**, *44*, 2538−2544.
(11) Zhang, J.; Huang, J.; Du, W.; Huang, F.; Du, L. Thermal Stability of the Copolymers of Silicon-Containing Arylacetylene Resin and Acetylene-Functional Benzoxazine. *Polym. Degrad. Stab.* **2011**, *96*, 2276−2283.
(12) Robertson, I. D.; Yourdkhani, M.; Centellas, P. J.; Aw, J. E.; Ivanoff, D. G.; Goli, E.; Lloyd, E. M.; Dean, L. M.; Sottos, N. R.; Geubelle, P. H.; Moore, J. S.; White, S. R. Rapid Energy-Efficient Manufacturing of Polymers and Composites via Frontal Polymerization. *Nature* **2018**, *557*, 223−227.
(13) Gautier, R.; Zhang, X.; Hu, L.; Yu, L.; Lin, Y.; Sunde, T. O. L.; Chon, D.; Poeppelmeier, K. R.; Zunger, A. Prediction and Accelerated Laboratory Discovery of Previously Unknown 18-Electron ABX Compounds. *Nat. Chem.* **2015**, *7*, 308.
(14) Bai, P.; Jeon, M. Y.; Ren, L.; Knight, C.; Deem, M. W.; Tsapatsis, M.; Siepmann, J. I. Discovery of Optimal Zeolites for Challenging Separations and Chemical Transformations Using Predictive Materials Modeling. *Nat. Commun.* **2015**, *6*, 5912.
(15) Mauro, J. C.; Tandia, A.; Vargheese, K. D.; Mauro, Y. Z.; Smedskjaer, M. M. Accelerating the Design of Functional Glasses through Modeling. *Chem. Mater.* **2016**, *28*, 4267−4277.
(16) Kim, C.; Chandrasekaran, A.; Huan, T. D.; Das, D.; Ramprasad, R. Polymer Genome: A Data-Powered Polymer Informatics Platform for Property Predictions. *J. Phys. Chem. C* **2018**, *122*, 17575−17585.
(17) Mannodi-Kanakkithodi, A.; Chandrasekaran, A.; Kim, C.; Huan, T. D.; Pilania, G.; Botu, V.; Ramprasad, R. Scoping the Polymer Genome: A Roadmap for Rational Polymer Dielectrics Design and Beyond. *Mater. Today* **2018**, *21*, 785−796.
(18) Huan, T. D.; Mannodi-Kanakkithodi, A.; Kim, C.; Sharma, V.; Pilania, G.; Ramprasad, R. A Polymer Dataset for Accelerated Property Prediction and Design. *Sci. Data* **2016**, *3*, 160012.
(19) Ramprasad, R.; Batra, R.; Pilania, G.; Mannodi-Kanakkithodi, A.; Kim, C. Machine Learning in Materials Informatics: Recent Applications and Prospects. *npj Comput. Mater.* **2017**, *3*, 54.
(20) Mannodi-Kanakkithodi, A.; Huan, T. D.; Ramprasad, R. Mining Materials Design Rules from Data: The Example of Polymer Dielectrics. *Chem. Mater.* **2017**, *29*, 9001−9010.
(21) Wang, Y.; Liu, Y.; Song, S.; Yang, Z.; Qi, X.; Wang, K.; Liu, Y.; Zhang, Q.; Tian, Y. Accelerating the Discovery of Insensitive High-Energy-Density Materials by a Materials Genome Approach. *Nat. Commun.* **2018**, *9*, 2444.
(22) Martin, R. L.; Simon, C. M.; Smit, B.; Haranczyk, M. In silico Design of Porous Polymer Networks: High-Throughput Screening for Methane Storage Materials. *J. Am. Chem. Soc.* **2014**, *136*, 5006−5022.
(23) Mäeorg, U.; Viirlaid, S.; Hagu, H.; Verkruijsse, H. D.; Brandsma, L. On the In Situ Trimethylsilylation of Zinc Acetylides. *J. Organomet. Chem.* **2000**, *601*, 341−342.
(24) Xu, J.-F.; Wang, C.-Y.; Lai, G.-Q.; Shen, Y.-J. Synthesis and Characterization of Phenylacetylene-Terminated Poly(silyleneethynylene-4,4′-phenylethereneethynylene)s. *Eur. Polym. J.* **2007**, *43*, 668−672.
(25) RDKit: Open Source Toolkit for Cheminformatics. http://www.rdkit.org/ (accessed May 10, 2020).
(26) PoLyInfo Database. http://polymer.nims.go.jp/index_en.html (accessed May 10, 2020).
(27) Fabig, S.; Haberhauer, G.; Gleiter, R. Dimerization of Two Alkyne Units: Model Studies, Intermediate Trapping Experiments, and Kinetic Studies. *J. Am. Chem. Soc.* **2015**, *137*, 1833−1843.
(28) Haberhauer, G.; Gleiter, R.; Fabig, S. Model Studies on the Dimerization of 1,3-Diacetylenes. *J. Org. Chem.* **2015**, *80*, 5077−5083.
(29) Bicerano, J. *Prediction of Polymer Properties*, 3rd ed.; Marcel Dekker Inc.: New York, 2002.
(30) Wang, C.; Zhou, Y.; Huang, F.; Du, L. Synthesis and Characterization of Thermooxidatively Stable Poly(dimethylsilyleneethynylenephenyleneethynylene) with O-Carborane Units. *React. Funct. Polym.* **2011**, *71*, 899−904.
(31) Wang, F.; Zhang, J.; Huang, J.; Yan, H.; Huang, F.; Du, L. Synthesis and Characterization of Poly(dimethylsilylene ethynylenephenyleneethynylene) Terminated with Phenylacetylene. *Polym. Bull.* **2006**, *56*, 19−26.
(32) Kruckenberg, T. M.; Paton, R. *Resin Transfer Moulding for Aerospace Structures*; Springer: Netherlands, 1998.
(33) Wessig, P.; Müller, G. The Dehydro-Diels-Alder Reaction. *Chem. Rev.* **2008**, *108*, 2051−2063.

(34) Gandon, S.; Mison, P.; Bartholin, M.; Mercier, R.; Sillion, B.; Geneve, E.; Grenier, P.; Grenier-Loustalot, M.-F. Thermal Polymerization of Arylacetylenes: 1. Study of a Monofunctional Model Compound. *Polymer* **1997**, *38*, 1439−1447.
(35) Gandon, S.; Mison, P.; Sillion, B. Thermal Polymerization of Arylacetylenes: 2. Study of Linear Dimers. *Polymer* **1997**, *38*, 1449−1459.
(36) Chen, Z.; Wang, L.; Lin, J.; Du, L. Theoretical Study on Thermal Curing Mechanism of Arylethynyl-Containing Resins. *Phys. Chem. Chem. Phys.* **2020**, *22*, 6468−6477.
(37) Menard, K. P. *Dynamic Mechanical Analysis: A Practical Introduction*; CRC Press: Boca Raton, 1999.
(38) Polymer Genome. http://www.polymergenome.org/ (accessed May 10, 2020).
(39) Guo, K.; Li, P.; Zhu, Y.; Wang, F.; Qi, H. Thermal Curing and Degradation Behaviour of Silicon-Containing Arylacetylene Resins. *Polym. Degrad. Stab.* **2016**, *131*, 98−105.
(40) Li, C.; Strachan, A. Molecular Scale Simulations on Thermoset Polymers: A Review. *J. Polym. Sci., Part B: Polym. Phys.* **2015**, *53*, 103−122.
(41) Venditti, R. A.; Gillham, J. K. A Relationship Between the Glass Transition Temperature ($T_g$) and Fractional Conversion for Thermosetting Systems. *J. Appl. Polym. Sci.* **1997**, *64*, 3−14.
(42) Gao, F.; Zhang, L.; Zhou, Y.; Huang, F.; Du, L. Synthesis and Characterization of Poly-[(methylsilyleneethynylenephenyleneethynylene)s-co-decamethylpentasiloxane]. *J. Macromol. Sci., Part A: Pure Appl.Chem.* **2010**, *47*, 861−866.
(43) Sifri, R. J.; Padilla-Vélez, O.; Coates, G. W.; Fors, B. P. Controlling the Shape of Molecular Weight Distributions in Coordination Polymerization and its Impact on Physical Properties. *J. Am. Chem. Soc.* **2020**, *142*, 1443−1448.
(44) Fabig, S.; Janiszewski, A.; Floß, M.; Kreuzahler, M.; Haberhauer, G. Dimerization of Substituted Arylacetylenes-Quantum Chemical Calculations and Kinetic Studies. *J. Org. Chem.* **2018**, *83*, 7878−7885.
(45) Whittle, M.; Gillet, V. J.; Willett, P.; Alex, A.; Loesel, J. Enhancing the Effectiveness of Virtual Screening by Fusing Nearest Neighbor Lists: A Comparison of Similarity Coefficients. *J. Chem. Inf. Model.* **2004**, *44*, 1840−1848.
(46) BIOVIA Materials Studio. https://www.3dsbiovia.com/products/collaborative-science/biovia-materials-studio/ (accessed May 10, 2020).
(47) Frisch, M. J.; Trucks, G. W.; Schlegel, H. B.; Scuseria, G. E.; Robb, M. A.; Cheeseman, J. R.; Scalmani, G.; Barone, V.; Mennucci, B.; Petersson, G. A.; et al. *Gaussian 09, Revision A.02*; Gaussian:Wallingford, CT, 2009.
(48) Xu, Z.; Lin, J.; Zhang, Q.; Wang, L.; Tian, X. Theoretical Simulations of Nanostructures Self-Assembled from Copolymer Systems. *Polym. Chem.* **2016**, *7*, 3783−3811.
(49) Jiang, T.; Wang, L.; Lin, J. Distinct Mechanical Properties of Nanoparticle-Tethering Polymers. *RSC Adv.* **2014**, *4*, 35272−35283.
(50) Yarovsky, I.; Evans, E. Computer Simulation of Structure and Properties of Crosslinked Polymers: Application to Epoxy Resins. *Polymer* **2002**, *43*, 963−969.
(51) Huang, F.; Lv, Y.; Wang, L.; Xu, P.; Lin, J.; Lin, S. An Insight into Polymerization-Induced Self-Assembly by Dissipative Particle Dynamics Simulation. *Soft Matter* **2016**, *12*, 6422−6429.
(52) Shenogina, N. B.; Tsige, M.; Patnaik, S. S.; Mukhopadhyay, S. M. Molecular Modeling Approach to Prediction of Thermo-Mechanical Behavior of Thermoset Polymer Networks. *Macromolecules* **2012**, *45*, 5307−5315.
(53) Radue, M. S.; Varshney, V.; Baur, J. W.; Roy, A. K.; Odegard, G. M. Molecular Modeling of Cross-Linked Polymers with Complex Cure Pathways: A Case Study of Bismaleimide Resins. *Macromolecules* **2018**, *51*, 1830−1840.
(54) Varshney, V.; Patnaik, S. S.; Roy, A. K.; Farmer, B. L. A Molecular Dynamics Study of Epoxy-Based Networks: Cross-Linking Procedure and Prediction of Molecular and Material Properties. *Macromolecules* **2008**, *41*, 6837−6842.
(55) Sun, H. COMPASS: An ab Initio Force-Field Optimized for Condensed-Phase ApplicationsOverview with Details on Alkane and Benzene Compounds. *J. Phys. Chem. B* **1998**, *102*, 7338−7364.


https://dx.doi.org/10.1021/acs.chemmater.0c00238
*Chem. Mater.* 2020, 32, 4527−4535